HHS Public Access

Author manuscript

Circulation. Author manuscript; available in PMC 2017 October 11.

Published in final edited form as:

Circulation. 2016 October 11; 134(15): 1085–1099. doi:10.1161/CIRCULATIONAHA.116.023003.

EXPERIMENTALLY INCREASING TITIN'S COMPLIANCE THROUGH RBM20 INHIBITION IMPROVES DIASTOLIC FUNCTION IN A MOUSE MODEL OF HFpEF

Mei Methawasin, MD, PhD, **Joshua G Strom, PhD**, **Rebecca E Slater, BS**, **Vanessa Fernandez, BS**, **Chandra Saripalli, MS**, and **Henk Granzier, PhD**

Department of Cellular and Molecular Medicine, University of Arizona, Tucson, AZ 85721; Sarver Molecular Cardiovascular Research Program, University of Arizona, Tucson, AZ 85721

Abstract

Background—Left Ventricular (LV) stiffening contributes to Heart Failure with preserved Ejection Fraction (HFpEF), a syndrome with no effective treatment options. Increasing titin's compliance in the heart has become possible recently through inhibition of the splicing factor RBM20. Here we investigated the effects of increasing titin's compliance in mice with diastolic dysfunction.

Methods—Mice in which the RNA recognition motif (RRM) of one of the RBM20 alleles was floxed and which expressed the MerCreMer transgene under control of the αMHC promoter (referred to as *cRbm20*$^{\Delta RRM}$ mice) were used. Mice underwent transverse aortic constriction (TAC) surgery and deoxycorticosterone acetate (DOCA) pellet implantation (TAC/DOCA). RRM deletion in adult mice was triggered by injecting raloxifene (*cRbm20*$^{\Delta RRM}$-raloxifene) with DMSO injected mice (*cRbm20*$^{\Delta RRM}$-DMSO) as the control. Diastolic function was investigated using echocardiography and pressure volume analysis; passive stiffness was studied in LV muscle strips and isolated cardiac myocytes before and after elimination of titin-based stiffness. Treadmill exercise performance was also studied. Titin isoform expression was evaluated with Agarose gels.

Results—*cRbm20*$^{\Delta RRM}$-raloxifene mice expressed large titins in the hearts, named super compliant titin (N2BAsc), which, within 3 weeks after raloxifene injection, made up ~45% of total titin. TAC/DOCA *cRbm20*$^{\Delta RRM}$-DMSO mice developed LV hypertrophy and a marked increase in LV chamber stiffness as shown by both pressure-volume analysis and echocardiography. LV chamber stiffness was normalized in TAC/DOCA *cRbm20*$^{\Delta RRM}$-raloxifene mice that expressed N2BAsc. Passive stiffness measurements on muscle strips isolated from the LV free wall revealed that extracellular matrix (ECM) stiffness was equally increased in both groups of TAC/DOCA mice (*cRbm20*$^{\Delta RRM}$-DMSO and *cRbm20*$^{\Delta RRM}$-raloxifene). However, titin-based muscle stiffness was reduced in the mice that expressed N2BAsc (TAC/DOCA *cRbm20*$^{\Delta RRM}$-raloxifene). Exercise

Address for Correspondence: Henk Granzier, PhD, Department of Molecular and Cellular Medicine, MRB 325. 1656 E Mabel Street., University of Arizona, Tucson, AZ-85724-5217. Voice: (520)6263641, FAX:(520)6267600, granzier@email.arizona.edu. H.G. is the Allan and Alfie Endowed Chair for Heart Disease in Women Research.

Conflict of Interest Disclosures

None

testing demonstrated significant improvement in exercise tolerance in TAC/DOCA mice that expressed N2BAsc.

Conclusions—Inhibition of the RBM20-based titin splicing system upregulates compliant titins, which improves diastolic function and exercise tolerance in the TAC/DOCA model. Titin holds promise as a therapeutic target for HFpEF.

Keywords

diastole; titin; HFpEF; RBM20; passive stiffness

INTRODUCTION

HFpEF is a complex clinical syndrome characterized by impairment in ventricular filling[12, 3]. The prevalence of HFpEF continues to grow but no treatment strategy has been proven to be effective[1, 4–6]. Increased diastolic LV stiffness is an important feature of HFpEF[2, 3, 7]. The two major contributors of LV passive stiffness are the extracellular matrix (ECM) and the cardiomyocytes, in which passive stiffness is mainly regulated by titin[3, 8, 9]. Increased titin stiffness has been shown to contribute to diastolic dysfunction in HFpEF[10–12]. Titin stiffness can be modulated through differential splicing (changes in titin isoform expression) and through posttranslational modification, primarily phosphorylation. Differential splicing pathways give rise to 2 adult cardiac titin isoforms with different size and stiffness: the N2B isoform (~3.0 MDa in size), and the N2BA isoform (~3.3 MDa). The N2BA/N2B titin isoform expression ratio increases during systolic heart failure[13, 14] which is thought to be a beneficial adaption to compensate for increased ECM-stiffness[13].

RNA binding motif-20 (RBM20) is a major splicing factor of titin[15–17]. The *Rbm20*$^{\Delta RRM}$ mouse model that has the RNA recognition motif (RRM) deleted has deficiency in titin splicing and expresses very large and compliant titin isoforms in the heart that result in increased LV chamber compliance[18]. The *Rbm20*$^{\Delta RRM}$ heterozygous mice have a normal life span and normal systolic function. Interestingly they also show enhanced exercise performance (relative to wild-type littermates)[18], suggesting a beneficial effect of increased LV chamber compliance. In this present study, we investigated the effect of increased titin compliance on chamber stiffness in pathological hearts.

Compliant titins were expressed through inhibiting RBM20 function and it was tested whether this ameliorates diastolic dysfunction. Diastolic dysfunction was induced by performing transverse aortic constriction (TAC) surgery with deoxycorticosterone acetate (DOCA) pellet implantation[19] and we used a conditional and cardiac-specific *Rbm20*$^{\Delta RRM}$ mouse model (αMHC MerCreMer *Rbm20*$^{\Delta RRM}$, or *cRbm20*$^{\Delta RRM}$ for short) to upregulate super compliant titin isoforms in the hearts of adult mice. TAC/DOCA mice have chronic pressure overload, increased oxidative stress, and are sensitized to mineralocorticoid excess, which accelerates adverse cardiac remodeling and promotes development of a HFpEF-like condition[1920]. We tested in TAC/DOCA mice whether upregulating compliant titin isoforms (*cRbm20*$^{\Delta RRM}$-raloxifene) ameliorates the HFpEF-like condition and studied its effect on LV diastolic stiffness, myocardial stiffness (ECM-based and titin-based) and exercise tolerance. We found that upregulating compliant titin has a highly beneficial effect on

diastolic function and exercise tolerance, supporting that titin is a potential therapeutic target for HFpEF.

METHODS

Additional details are in the Supplemental Methods.

Mice

Rbm20$^{\Delta RRM}$ mice which had exons 6 and 7 of *Rbm20* flanked with LoxP sites and which expressed MerCreMer recombinase protein under transcriptional control of the α-myosin heavy chain (MHC6) promoter were used[21]. Mice were heterozygous for the mutant RBM20 allele and for the MerCreMer transgene. For simplicity sake, we refer to these mice as *cRbm20*$^{\Delta RRM}$. We used male 8 week old mice on a C57BL/6J background. All experiments were approved by the University of Arizona Institutional Animal Care and Use Committee and followed the U.S. National Institutes of Health *Using Animals in Intramural Research* guidelines for animal use.

Experimental protocol

A schematic of the protocol is in Figure 1A. A preoperative echo was performed to obtain baseline cardiac parameters, then TAC/DOCA surgery was conducted to induce a HFpEF-like state. Minimally invasive transverse aortic constriction (TAC) was performed as described previously[22] with modifications. The aortic banding procedure used a 27-gauge needle to constrict the aorta. A deoxycorticosterone acetate (DOCA) 50 mg/pellet, 21 day release was implanted subcutaneously at the time of TAC. At 1 week post-surgery, post-constrictional aortic pressure gradient was measured to quantify the severity of constriction. Mice were then randomly divided into two groups that had an identical mean constrictional aortic pressure gradient (Figure S1). One of the groups was injected with raloxifene (dissolved in DMSO, 40 μg/gm body weight) and the other with DMSO only (same volume as first group). Intraperitoneal injection occurred daily for 8 consecutive days. We used as an additional control group *cRbm20*$^{\Delta RRM}$ mice that underwent a sham TAC/DOCA operation. Sham animals underwent the same procedure except the aorta was not ligated, a placebo pellet was implanted, and DMSO (vehicle) was injected one week after the sham surgery. At 2 weeks post-surgery, a follow up echocardiography study was performed to evaluate diastolic function (pilot studies had revealed that at this time titin expression was normal but that mice were in diastolic dysfunction). At 4 weeks post-surgery, a final echocardiography was performed, then the mice were used for PV analysis, isolated cardiomyocyte studies, LV wall passive stiffness measurement and protein analysis.

Echocardiography

Echocardiography was performed as previously described[18, 23] using a Vevo 2100 Imaging System (Visual-Sonics). Standard imaging planes, M-mode, Doppler, and functional calculations were obtained according to American Society of Echocardiography guidelines. The heart rate during echocardiographic study was maintained in the range of 500 –550 beats/minute for M-mode, 450–500 beats/minute for B-mode and 350 to 450 beats/minute for Doppler studies.

Pressure-Volume analysis

In vivo pressure-volume measurements were obtained with an admittance-based system (SciSense) in anesthetized ventilated mice. The IVC was located and occluded during a sigh (pause) in ventilation to acquire load-independent indexes. Data acquisition and analysis was performed in LabScribe2 (iWorx, Dover NH). EDPVR was analyzed using a monoexponential fit ($P = C + Ae^{\beta V}$) with the exponent (β) reported as the stiffness[24].

Exercise testing

Mice were tested using a 6 lane rodent treadmill system at progressively increasing speeds. Maximal speed and running distance were determined.

Isolated cardiomyocyte passive stiffness

Cells were isolated as described previously[25] and skinned cardiac myocyte mechanics were as in[26].

LV free wall passive stiffness

Mid-myocardial fibers (circumferential orientation) from LV free wall were carefully dissected and skinned. Relaxed fibers were stretched 1 base length/sec from their slack length to predetermined sarcomere lengths. To determine the collagen contribution to passive stress, thick and thin filaments were extracted from the sarcomere, removing titin's anchors in the sarcomere[9, 27]. Stress measurements after extraction were ECM-based and titin-based values were taken to be the difference in values before and after extraction. In order to determine stiffness the derivative of the passive stress equation was used.

Picrosirius red (PSR) staining

Picrosirius red (PSR) stained sections were used to measure the collagen volume fraction in LV cross-sections.

In-vivo cellular dimensions and SL measurement

The hearts were arrested with a Krebs solution containing high KCl (35 mM) and BDM 2,3-butanedione monoxide (20 mM) and the LV was vented, to ensure that the LV chamber was in diastasis during fixation. The hearts were sectioned transversely and sections were stained by anti-laminin to detect the lateral cell border, anti-connexin43 to detect intercalated discs and anti α-actinin to stain Z-disks. Cells in longitudinally sectioned mid-myocardial fibers that run circumferentially along the LV wall were studied to determined cell length, cell width, cell area and sarcomere length.

Protein analysis

Titin isoform analysis was performed with standard Agarose electrophoresis[28] and protein expression levels were quantified with western blotting as previously described[29].

Statistical analysis

Statistical analysis was performed in Graphpad Prism (GraphPad Software, Inc) and results are shown as mean ± SEM, with the details of the statistical tests used in each of the figures

and tables provided in the Supplemental Methods, Statistical Analysis section. The significance levels are shown on the Figures and in the legends of the Figures and Tables. The number of animals or cells in each group are shown in the legends of the figures and tables in the following order: sham, TAC/DOCA *cRbm20*$^{\Delta RRM}$-DMSO and TAC/DOCA *cRbm20*$^{\Delta RRM}$-raloxifene.

RESULTS

The hypothesis that experimentally increasing titin's compliance through inhibition of the titin splicing factor RBM20 ameliorates diastolic dysfunction was tested. First a model was developed in which compliant titin can be expressed in a cardiac specific and inducible manner, the *cRbm20*$^{\Delta RRM}$ model. To induce diastolic dysfunction a previously published procedure was used that creates a HFpEF-like state in the mouse, by mildly increasing afterload on the heart through transverse aortic constriction (TAC) with concomitant deoxycorticosterone acetate (DOCA) administration[19]. Exercise tolerance tests were performed and diastolic function and LV stiffness were studied using serial echocardiography, PV analysis, cardiomyocyte and LV wall muscle mechanics.

Expression of N2BAsc titins in *cRbm20*$^{\Delta RRM}$ mice

The time course and efficacy of raloxifene to trigger expression of large titin isoforms was studied by inducing Cre-mediated RBM20 inhibition in the *cRbm20*$^{\Delta RRM}$ mouse model. Raloxifene was administered to c*Rbm20*$^{\Delta RRM}$ mice, and the animals were sacrificed at different time points for titin isoform analysis. Titin expression was normal one week after the start of raloxifene injection (Figure 1B middle lane), but as time progressed 2 large titin isoforms appeared with an estimated molecular weight of ~3.5 and ~3.6 MDa (Figure 1B, right lane). It is known from previous work with a *conventional Rbm20*$^{\Delta RRM}$ model that these large isoforms are N2BA type titins (i.e., they contain the N2B and N2A elements) and that they are larger than normal because they express many additional spring element exons, which is reflected in their increased compliance[18]. Hence the two large N2BA titins are referred to as super compliant N2BA titin (N2BAsc). A significant amount of N2BAsc titins was detected as early as 2 weeks after starting the raloxifene injections and the ratio of N2BAsc / total titin reached ~ 0.45 at week 3, and then plateaued (Figure 1C). While N2BAsc titins increased, adult N2B and N2BA titins decreased over time so that total expression level of titin did not change (Table S1). *cRbm20*$^{\Delta RRM}$ mice that were injected with vehicle (DMSO) expressed normal adult titin isoforms (Figure 1B). Thus, the *cRbm20*$^{\Delta RRM}$ mouse model is an ideal tool to increase titin's compliance in the heart.

TAC/DOCA mice exhibit diastolic dysfunction

Three groups of *cRbm20*$^{\Delta RRM}$ mice were studied, two of which underwent the TAC/DOCA procedure and the third group underwent a sham surgery (Methods). The *cRbm20*$^{\Delta RRM}$ groups were injected one week after the surgery, one group with raloxifene and the other two (sham and TAC/DOCA) with DMSO only. One week later all mice were studied via echocardiography. At this time point raloxifene had not yet induced significant expression of N2BAsc (Figure 1C). Echocardiography showed that both TAC/DOCA groups had developed LV concentric hypertrophy and that they had a significant left atrial (LA)

enlargement (Table S2). (Examples of raw data are shown in Supplemental Figure S1). Trans-mitral Doppler flow velocity showed a more rapid deceleration of the mitral E wave (Fig. 2A, top), suggesting an increase in LV chamber stiffness[30, 31]. The ratio of mitral E velocity to mitral annular e' velocity (E/e'), a reliable predictor of LV end diastolic pressure (LVEDP)[32, 33], was elevated in both TAC/DOCA groups (Fig. 2B, top). The ratio of mitral E/A velocity was increased, also suggesting a restrictive LV filling pattern, while the ejection fraction (EF) was preserved (Fig. 2C and D, top). In summary, 2 weeks post TAC/DOCA surgery, both TAC/DOCA groups developed a similar degree of diastolic dysfunction while systolic function was preserved. The diastolic dysfunction, concentric hypertrophy, and normal systolic function are consistent with previous work[19] and support that the TAC/DOCA procedure in the mouse creates a HFpEF-like state.

Expressing N2BAsc titins ameliorates diastolic dysfunction

The same 3 groups of *cRbm20*$^{\Delta RRM}$ mice were studied again 4 weeks after TAC/DOCA surgery (or 3 weeks after administering raloxifene), a time point at which an approximate constant level of N2BAsc titins was expressed in the heart (Figure S2 shows titin isoform expression at this time point, as well as RBM20 expression data). Transmitral Doppler echo showed that TAC/DOCA *cRbm20*$^{\Delta RRM}$-DMSO mice continued to have diastolic dysfunction (reduced mitral E deceleration times and increased E/e' and E/A ratios). However, all of these parameters were normalized in *cRbm20*$^{\Delta RRM}$–raloxifene mice (Figure 2 bottom row). The ejection fraction remained normal in all groups (Fig. 2D, bottom).

A pressure-volume (PV) analysis was also performed at the 4 week post-surgery time point (representative loops are shown in Figure 3A). This revealed an increase in end systolic pressure (ESP) as well as arterial elastance (Ea) in both TAC/DOCA groups (Table 1) consistent with the increased afterload due to the transverse aortic constriction. The diastolic stiffness coefficient (β) of the end diastolic pressure volume relation (EDPVR), which reflects LV chamber stiffness, was increased in the TAC/DOCA *cRbm20*$^{\Delta RRM}$-DMSO group, but was normalized in the raloxifene group (Figure 3B). Left ventricular end diastolic pressure (LVEDP), a predictor of decompensated heart failure, was elevated in the DMSO group but was normal in raloxifene mice (Figure 3C). In addition, the LV relaxation time constant (Tau Glantz) was prolonged in the TAC/DOCA *cRbm20*$^{\Delta RRM}$-DMSO mice, suggesting impaired LV relaxation, but Tau Glantz was normal in raloxifene mice (Table 1). Thus, results from the PV analysis revealed that TAC/DOCA mice exhibit slowed LV relaxation and increased LV chamber stiffness and, importantly, that expression of N2BAsc improves LV relaxation and increased LV chamber compliance.

Although titin is the main target of RBM20, previous studies in the *conventional Rbm20*$^{\Delta RRM}$ model showed that in heterozygous mice (the genotype that was studied in the present work) two additional genes are alternatively spliced: CaMKIIδ and Ldb3/Cypher[18]. These two genes were studied at the protein level. For CaMKIIδ, its total expression level was found to be unaltered in *cRbm20*$^{\Delta RRM}$–raloxifene relative to *cRbm20*$^{\Delta RRM}$–DMSO groups and of the known CaMKIIδ targets (S282 in cMyBP-C, Thr17 in PLB, and p53) none were different between the raloxifene and DMSO groups (Figure S3A–D), consistent with the previous results in the conventional model[18]. Additionally, there were no changes in

Ca^{2+} transients measured in single cardiac myocytes (Figure S4). As for the short and long cardiac isoforms of LDB3, no differences were found (Figure S3 E, F). Thus it is likely that exon expression changes and their functional consequences in *cRbm20*$^{\Delta RRM}$–raloxifene mice are largely restricted to titin. Finally, as an additional control the effects of raloxifene or DMSO administered to *cRbm20*$^{\Delta RRM}$ mice that had not undergone TAC/DOCA surgery was studied. No differences in cardiac function were present 1 and 3 weeks after the injection (Table S3). Thus obtained results are specific to the TAC/DOCA state with RBM20 inhibition. In summary, partially inactivating RBM20 by administering raloxifene in *cRbm20*$^{\Delta RRM}$ TAC/DOCA mice specifically upregulates compliant titins (N2BAsc), and is highly effective in normalizing diastolic function.

Mechanistic basis for diastolic function recovery in *cRbm20*$^{\Delta RRM}$ TAC/DOCA mice

To address the mechanism of improved diastolic function in mice that express N2BAsc, the contribution of extracellular matrix (ECM) to LV chamber stiffness was first studied. Considering that TAC/DOCA is known to cause myocardial fibrosis[19, 34], RBM20 inhibition might reduce fibrosis and explain the increased chamber compliance in raloxifene mice. We therefore studied passive stiffness of muscle strips dissected from the LV free wall, to determine the contribution of the ECM to myocardial stiffness. ECM-based stiffness was measured after thick and thin filament extraction, which removes the anchors of titin in the sarcomeres, leaving only the ECM-based stiffness component[27]. Passive stiffness was determined as the derivative of the passive stress vs sarcomere length relation (Methods). Results showed that ECM-based passive stiffness was increased in both TAC/DOCA groups (Figure 4A). (The total passive stiffness and the stiffness differences before and after extraction (due to titin) are shown in Supplemental Figure S5.) We used Picrosirius Red (PSR) staining to quantify myocardial fibrosis in LV myocardium of TAC/DOCA mice (example results are shown in Fig. 4B) and determined from this the collagen volume fraction, collagen fiber length and collagen fiber width. All collagen parameters were increased in both TAC/DOCA groups relative to the sham group with no difference between DMSO and raloxifene mice (Figure 4C–E). In summary, results showed that ECM-based passive stiffness was similarly increased in both TAC/DOCA groups and that consistent with this finding collagen is similarly upregulated in both groups. This indicates that the lower LV chamber stiffness in *cRbm20*$^{\Delta RRM}$-raloxifene mice is not readily explained by a reduction in myocardial fibrosis.

Passive stiffness of demembraned (skinned) cardiomyocytes was studied next. LV cardiomyocytes of TAC/DOCA *cRbm20*$^{\Delta RRM}$-DMSO mice had high passive stiffness, while LV cardiomyocytes of *cRbm20*$^{\Delta RRM}$-raloxifene mice had passive stiffness that was slightly less than that of sham mice (Figures 5A). LV cardiomyocytes of *cRbm20*$^{\Delta RRM}$-raloxifene mice had longer slack sarcomere lengths (SL) (Figure 5B) consistent with expression of N2BAsc titins in the sarcomeres (see Discussion). The passive myocyte mechanics suggests that the lower LV chamber stiffness in the *cRbm20*$^{\Delta RRM}$- raloxifene group might be due, at least in part, to the reduced passive stiffness of cardiomyocytes.

We also studied the size of cardiomyocytes and sarcomere length in the LV of hearts fixed at diastasis, using confocal microscopy (Figure 6A shows examples). This revealed an

enlargement of cardiomyocytes in longitudinal and radial dimensions of both TAC/DOCA groups (Fig. 6B), consistent with their hypertrophic phenotype observed at the LV chamber level (Table 1). However, cardiomyocytes of TAC/DOCA *cRbm20*$^{\Delta RRM}$-raloxifene mice were slightly smaller in the radial direction than those of TAC/DOCA *cRbm20*$^{\Delta RRM}$-DMSO mice: the cell width was reduced from 27.8 to 26.6 μm. Although the cell length was not different in the two TAC/DOCA groups, the number of sarcomeres per cell length, calculated from the mean cell length and mean SL, was reduced from 65 in the DMSO group to 61 in the raloxifene group (Fig. 6B). These cell studies suggest an attenuated hypertrophic response in the presence of compliant N2BAsc (see also Discussion).

Exercise tolerance

Whether the lower diastolic stiffness of TAC/DOCA *cRbm20*$^{\Delta RRM}$–raloxifene mice was functionally beneficial was studied next. The running distance was studied in a treadmill running test that exposed the mice to a progressively increasing speed (Methods). The treadmill test was performed three times: preoperative and at 2 weeks and at 4 weeks post TAC/DOCA surgery. The running distance was recorded and calculated as a percent of the preoperative running distance of each individual mouse (Figure 7A). At 2 weeks post-surgery, both groups of TAC/DOCA mice had a reduction in running distance, which correlated with the echo results indicating that both groups of mice had developed diastolic dysfunction. At 4 weeks post-surgery while the running distance of *cRbm20*$^{\Delta RRM}$-DMSO mice remained diminished the *cRbm20*$^{\Delta RRM}$-raloxifene showed an increased running distance back to a level comparable to sham mice (Figure 7B), indicating recovery of exercise intolerance.

DISCUSSION

The effects of expressing compliant titins was studied in mice with diastolic dysfunction. A mouse model was used with HFpEF-like characteristics, achieved by inducing pressure overload (TAC) with concomitant mineralocorticoid supplementation (DOCA). We studied whether upregulating compliant titin isoforms lessened HFpEF symptoms by performing the TAC/DOCA procedure in *cRbm20*$^{\Delta RRM}$ mice and then inhibiting RBM20. This resulted in noticeable expression of compliant titin isoforms (N2BAsc) within two weeks and near maximal expression within 3 weeks. When expression of N2BAsc titin was triggered in mice in a HFpEF-like state, normalization in diastolic function and improvement in exercise tolerance ensued. Below these findings are discussed in detail.

Creating a mouse model with HFpEF-like symptoms

The TAC/DOCA method was previously described by Mohammed et al.[19] who demonstrated that mineralocorticoid excess (DOCA) in the presence of chronic mild pressure overload (TAC) causes LV hypertrophy, fibrosis and diastolic dysfunction[19]. We used this method and, consistent with previous work, found that the mitral valve E wave deceleration time was reduced and that the ratio of mitral inflow (E) to late atrial kick (A) was enhanced. Additionally, the ratio of mitral E velocity to mitral annular e' velocity (E/e'), a predictor of LV end diastolic pressure (LVEDP)[32, 33], was increased. These echo parameters indicate that TAC/DOCA causes diastolic dysfunction. This conclusion is

supported by a pressure volume analysis that revealed elevated LVEDP and an increase in diastolic stiffness coefficient (β) of the end diastolic pressure volume relation. Thus the TAC/DOCA mice are in diastolic dysfunction. This -- combined with slowed LV chamber relaxation, increased lung weights, impaired exercise capacity, and normal ejection fraction (Tables 1 and S2) -- supports that the TAC/DOCA method creates a HFpEF-like condition in the mouse.

The underlying basis for increased diastolic stiffness in TAC/DOCA mice includes both increased passive stiffness of the ECM (increased fibrosis and increased ECM stiffness (Figures 4A)) and increased passive stiffness of cardiac myocytes (Figures 5A). The increased cellular passive stiffness is likely derived from post-translational modification on titin as isoform analysis did not reveal changes in the N2B:N2BA expression ratio (Figure S2A), a conclusion similar to that drawn in a recent study on biopsies from HFpEF patients[11]. Thus the TAC/DOCA model is a well-suited HFpEF-like mouse model for testing therapeutic approaches.

Expression of compliant titin isoforms (N2BAsc) lowers titin-based passive stiffness

To manipulate titin's stiffness back towards normal we took advantage of the recent discovery that inactivation of the splicing factor RBM20 results in expression of large titin isoforms[15–17]. In the present work we used a conditional version of the previously published *Rbm20*$^{\Delta RRM}$ model[18], and, through crossing this conditional model with the αMHC-MerCreMer mouse, created an inducible cardiac-specific *Rbm20*$^{\Delta RRM}$ mouse. The *conventional Rbm20*$^{\Delta RRM}$ model was previously characterized with a genome-wide exon expression array[18]. This established that titin exons greatly dominate the differentially expressed exons, with two additional genes that were alternatively spliced in Het mice, Ldb3/Cypher and CaMKIIδ. We evaluated these two genes in TAC/DOCA *cRbm20*$^{\Delta RRM}$–raloxifene mice and found no differences in their expression levels or in the downstream CaMKIIδ targets[18] (e.g., cMyBP-C, PLB, and p53, Figure S3) as compared to TAC/DOCA *cRbm20*$^{\Delta RRM}$–DMSO. It is likely, therefore, that the changes in exon expression and their functional consequences in *cRbm20*$^{\Delta RRM}$–raloxifene mice are dominated by titin.

The difference in titin-based passive stiffness between *cRbm20*$^{\Delta RRM}$–raloxifene and *cRbm20*$^{\Delta RRM}$–DMSO is large (as per Figure 5A, a 50% reduction at SL 2.15 μm) and we evaluated whether this can be explained by expression of N2BAsc as follows. The previous exon expression analysis on myocardium of *conventional Rbm20*$^{\Delta RRM}$ Het mice had shown that changes in exon expression were restricted to titin's spring region where 34 exons in the tandem immunoglobulin segment and 10 exons in the PEVK region were upregulated[18]. Although a similar exon expression analysis was not performed in the present study, considering that this new model also targets the RRM (*Rbm20* exons 6 and 7 were floxed) it is likely that the modification in titin will be the same as well. This notion is consistent with the indistinguishable mobility of the N2BAsc isoforms expressed in the LV of the conventional and conditional *Rbm20*$^{\Delta RRM}$ mice (data not shown). The functional consequence of upregulating spring element exons is an increase in the contour length of the spring region: the tandem Ig segment by 34 × ~5 nm (increase due to Ig domain upregulation, with an estimated domain spacing of ~ 5 nm) and the PEVK region by 300×

0.35 nm (the number of upregulated amino acid residues times their maximal residue spacing of ~0.35 nm)[35]. This increased contour length explains the increased slack sarcomere length that was found (Fig. 5B). It is also expected to lower passive force at a given degree of sarcomere stretch, due to the lower fractional extension of the spring region (compared to the N2B titin isoform). Using single molecule spring element characteristics we simulated the force produced by N2B titin and N2BAsc as a function of sarcomere length (SL) and converted this to a passive stiffness-SL relation. We found that the stiffness reduction that results from the titin spring element exon upregulation is large (Figure S6) and is 89% at a SL of 2.15 μm (selected because this is likely a physiological SL as is suggested by work on hearts fixed in diastole[8] and the elegant work of Kobirumaki-Shimozawa and colleagues who imaged sarcomere length in vivo in the living animal[36]). Since in the heart not all N2B titin is converted to N2BAsc but only 45% (calculated from Table S1, at 3 wk time point) the predicted stiffness reduction is 40%. This calculated stiffness reduction is relatively close to the measured 50% reduction (Fig. 5A) especially considering the uncertainty in some of the input parameters of the calculation (see Caption of Figure S6). In summary, expressing N2BAsc titins is highly effective in lowering cardiac myocyte passive stiffness.

In vivo cardiomyocyte morphology revealed that the width of *cRbm20*$^{\Delta RRM}$–raloxifene cells was reduced compared to *cRbm20*$^{\Delta RRM}$–DMSO cells (Fig. 6B), consistent with the normalization of the LV wall thickness and LV concentricity of the *cRbm20*$^{\Delta RRM}$–raloxifene mice (Table 1). Attenuated concentric LV hypertrophy is likely to be a beneficial response as it is expected to accommodate more blood volume during diastolic filling. The cell morphology study also indicates that in the raloxifene group the number of serially-linked sarcomeres was reduced, further supporting a hypertrophy reduction. The attenuated hypertrophy in response to pressure overload in the *cRbm20*$^{\Delta RRM}$–raloxifene mice that express super complaint titins might have multiple underlying mechanisms and future work is needed to address them. This should include a focus on titin-based signaling as our findings are consistent with the widely held hypothesis in the field[37–40] that titin functions as a mechanosensor that senses titin's I-band strain and controls hypertrophic signaling.

Expressing N2BAsc titins improves diastolic function and exercise capacity

Primary findings of our work are that expressing N2BAsc in mice with HFpEF-like symptoms normalizes diastolic stiffness, as revealed by echocardiography and pressure-volume analysis (Table 1), and that improves exercise performance (Figure 7). These positive effects take place despite continued fibrosis and elevated ECM-based stiffness, indicating that the reduced titin-based stiffness is a dominant effect. Expressing N2BAsc did not reverse anatomical remodeling of LV and LA chambers at 4 weeks post-surgery (Table 1). This might be explained by the continued pressure overload (the aortic constriction was not removed) or insufficient time for reversal of anatomical remodeling to take place[41–44]. The latter is supported by results from a pilot study in which TAC/DOCA *cRbm20*$^{\Delta RRM}$ mice were sacrificed 14 weeks after raloxifene injection and that showed normalization of left atrial dimension, as well as diastolic function recovery (results not shown). In addition to the beneficial effect of RBM20 inactivation on diastolic stiffness, the isovolumic relaxation constant (Tau glanz) of the LV chamber that was increased in TAC/DOCA mice (slowed

relaxation) was normalized when N2BAsc were expressed (Table 1). Surprisingly, the Ca^{2+} transients of isolated intact cardiomyocyte were not different when comparing TAC/DOCA mice without and with N2BAsc expression (Figure S4). Thus the improvement in relaxation of the LV chamber cannot be readily explained by enhanced Ca^{2+} reuptake kinetics. Instead we propose that the explanation resides within the myofilaments. Studies with the *conventional Rbm20*$^{\Delta RRM}$ mice have shown that expression of N2BAsc results in a reduction in the Ca^{2+} sensitivity of force development and an increase in the apparent detachment rate constant of force generating crossbridges (*g*app)[18], both of which are expected to speed relaxation. In summary, expression of compliant titin isoforms (N2BAsc) in mice with HFpEF-like symptoms reduces diastolic chamber stiffness, facilitates LV relaxation and improves exercise capacity.

Clinical implications

No effective therapies exists for treating HFpEF patients and a recent clinical trial that sought to lower titin's pathological stiffness in HFpEF patients by normalizing posttranslational modifications on titin (summarized in the recent RELAX trial)[45] was not successful as clinical outcomes and exercise capacity did not improve[46]. Our work suggests that an alternative therapeutic approach might be the upregulation of compliant titin isoforms, thereby improving diastolic function and improving exercise capacity. Can our findings in the mouse be extrapolated to humans? The expression ratio of the adult titin isoforms varies amongst species and in the mouse LV the N2B: N2BA ratio is ~80:20, while in humans this ratio is ~65:35[11]. When N2BAsc replaces N2B titin the passive stiffness reduction will be larger than when replacing N2BA titin (because N2B titin is stiffer than N2BA titin) and thus the stiffness reduction in human is expected to be somewhat less than in the mouse. Performing an analysis analogous to the one shown in Figure S6 and assuming a similar ~40% RBM20 inhibition as achieved in the mouse (Fig. S2B) we estimate that at an SL of 2.15 μm the passive stiffness reduction in humans would be 33% (as opposed to 40% in the mouse). It is likely that this would invoke considerable functional benefits and, thus, upregulating compliant titin as a HFpEF therapy seems a worthwhile pursuit. Genetically targeting *Rbm20* is relatively straightforward in the mouse, but is extremely challenging in humans and instead developing small molecule inhibitors that specifically target binding of RBM20 to titin transcript are more likely to be successful. Cardiac-specificity of such inhibitor would be ideal, but since we have not found a functional defect caused by upregulating compliant titin isoforms in skeletal muscle (based on our work with the *conventional Rbm20*$^{\Delta RRM}$ mouse) cardiac specificity might not be essential. Since cardiac RBM20 expression levels vary amongst individuals[47], the precise level of RBM20 inhibition required to have an ideal beneficial effect on diastolic function may vary among patients and might require careful dosing according to the underlying cardiac pathology and stage of heart failure.

The promise of targeting titin is revealed by the improved exercise performance of mice that express N2BAsc titins, a finding that might be due to the increase in ventricular chamber compliance and a more rapid active myocardial relaxation that is expected to result in a larger end-diastolic volume and a higher cardiac output during exercise. The increased exercise performance of mice that express N2BAsc is consistent with the study of Nagueh et

al[13] that showed a positive correlation between the N2BA(compliant):N2B(stiff) isoform ratio and peak oxygen consumption (VO2) in human heart failure patients. The enhanced exercise performance of both ‘mice and men’ that express compliant titins shows that inhibiting the RBM20-based titin splicing system should be considered as a strategy for improving cardiac function in HFpEF patients. Titin holds great promise as a therapeutic target for HFpEF.

Supplementary Material

Refer to Web version on PubMed Central for supplementary material.

Acknowledgments

We are grateful to our lab members and acknowledge the University of Arizona Genetic Engineering of Mouse Models (GEMM) and Mouse Phenotyping Core Facilities.

Funding

National Institutes of Health HL062881 and HL118524, and Foundation Leducq (TNE-13CVD04) (H.L.).

References

1. Borlaug BA. The pathophysiology of heart failure with preserved ejection fraction. Nat Rev Cardiol. 2014; 11:507–515. [PubMed: 24958077]
2. van Heerebeek L, Franssen CP, Hamdani N, Verheugt FW, Somsen GA, Paulus WJ. Molecular and cellular basis for diastolic dysfunction. Current heart failure reports. 2012; 9:293–302. [PubMed: 22926993]
3. Borlaug BA, Paulus WJ. Heart failure with preserved ejection fraction: Pathophysiology, diagnosis, and treatment. Eur Heart J. 2011; 32:670–679. [PubMed: 21138935]
4. Lewinter MM, Meyer M. Mechanisms of diastolic dysfunction in heart failure with a preserved ejection fraction: If it's not one thing it's another. Circulation. Heart failure. 2013; 6:1112–1115. [PubMed: 24255055]
5. Basaraba JE, Barry AR. Pharmacotherapy of heart failure with preserved ejection fraction. Pharmacotherapy. 2015; 35:351–360. [PubMed: 25884524]
6. Nanayakkara S, Kaye DM. Management of heart failure with preserved ejection fraction: A review. Clin Ther. 2015; 37:2186–2198. [PubMed: 26385583]
7. Paulus WJ, Tschope C. A novel paradigm for heart failure with preserved ejection fraction: Comorbidities drive myocardial dysfunction and remodeling through coronary microvascular endothelial inflammation. Journal of the American College of Cardiology. 2013; 62:263–271. [PubMed: 23684677]
8. Chung CS, Granzier HL. Contribution of titin and extracellular matrix to passive pressure and measurement of sarcomere length in the mouse left ventricle. J Mol Cell Cardiol. 2011; 50:731–739. [PubMed: 21255582]
9. Granzier HL, Irving TC. Passive tension in cardiac muscle: Contribution of collagen, titin, microtubules, and intermediate filaments. Biophys J. 1995; 68:1027–1044. [PubMed: 7756523]
10. Borbely A, van der Velden J, Papp Z, Bronzwaer JG, Edes I, Stienen GJ, Paulus WJ. Cardiomyocyte stiffness in diastolic heart failure. Circulation. 2005; 111:774–781. [PubMed: 15699264]
11. Zile MR, Baicu CF, Ikonomidis J, Stroud RE, Nietert PJ, Bradshaw AD, Slater R, Palmer BM, Van Buren P, Meyer M, Redfield M, Bull D, Granzier H, LeWinter MM. Myocardial stiffness in patients with heart failure and a preserved ejection fraction: Contributions of collagen and titin. Circulation. 2015; 131:1247–1259. [PubMed: 25637629]

12. Borbely A, Falcao-Pires I, van Heerebeek L, Hamdani N, Edes I, Gavina C, Leite-Moreira AF, Bronzwaer JG, Papp Z, van der Velden J, Stienen GJ, Paulus WJ. Hypophosphorylation of the stiff n2b titin isoform raises cardiomyocyte resting tension in failing human myocardium. Circ Res. 2009; 104:780–786. [PubMed: 19179657]

13. Nagueh SF, Shah G, Wu Y, Torre-Amione G, King NM, Lahmers S, Witt CC, Becker K, Labeit S, Granzier HL. Altered titin expression, myocardial stiffness, and left ventricular function in patients with dilated cardiomyopathy. Circulation. 2004; 110:155–162. [PubMed: 15238456]

14. Makarenko I, Opitz CA, Leake MC, Neagoe C, Kulke M, Gwathmey JK, del Monte F, Hajjar RJ, Linke WA. Passive stiffness changes caused by upregulation of compliant titin isoforms in human dilated cardiomyopathy hearts. Circ Res. 2004; 95:708–716. [PubMed: 15345656]

15. Greaser ML, Krzesinski PR, Warren CM, Kirkpatrick B, Campbell KS, Moss RL. Developmental changes in rat cardiac titin/connectin: Transitions in normal animals and in mutants with a delayed pattern of isoform transition. J Muscle Res Cell Motil. 2005; 26:325–332. [PubMed: 16491431]

16. Greaser ML, Warren CM, Esbona K, Guo W, Duan Y, Parrish AM, Krzesinski PR, Norman HS, Dunning S, Fitzsimons DP, Moss RL. Mutation that dramatically alters rat titin isoform expression and cardiomyocyte passive tension. J Mol Cell Cardiol. 2008; 44:983–991. [PubMed: 18387630]

17. Guo W, Schafer S, Greaser ML, Radke MH, Liss M, Govindarajan T, Maatz H, Schulz H, Li S, Parrish AM, Dauksaite V, Vakeel P, Klaassen S, Gerull B, Thierfelder L, Regitz-Zagrosek V, Hacker TA, Saupe KW, Dec GW, Ellinor PT, MacRae CA, Spallek B, Fischer R, Perrot A, Ozcelik C, Saar K, Hubner N, Gotthardt M. Rbm20, a gene for hereditary cardiomyopathy, regulates titin splicing. Nat Med. 2012; 18:766–773. [PubMed: 22466703]

18. Methawasin M, Hutchinson KR, Lee EJ, Smith JE 3rd, Saripalli C, Hidalgo CG, Ottenheijm CA, Granzier H. Experimentally increasing titin compliance in a novel mouse model attenuates the frank-starling mechanism but has a beneficial effect on diastole. Circulation. 2014; 129:1924–1936. [PubMed: 24599837]

19. Mohammed SF, Ohtani T, Korinek J, Lam CS, Larsen K, Simari RD, Valencik ML, Burnett JC Jr, Redfield MM. Mineralocorticoid accelerates transition to heart failure with preserved ejection fraction via "nongenomic effects". Circulation. 2010; 122:370–378. [PubMed: 20625113]

20. Yancy CW, Jessup M, Bozkurt B, Butler J, Casey DE Jr, Drazner MH, Fonarow GC, Geraci SA, Horwich T, Januzzi JL, Johnson MR, Kasper EK, Levy WC, Masoudi FA, McBride PE, McMurray JJ, Mitchell JE, Peterson PN, Riegel B, Sam F, Stevenson LW, Tang WH, Tsai EJ, Wilkoff BL. 2013 accf/aha guideline for the management of heart failure: Executive summary: A report of the american college of cardiology foundation/american heart association task force on practice guidelines. Circulation. 2013; 128:1810–1852. [PubMed: 23741057]

21. Sohal DS, Nghiem M, Crackower MA, Witt SA, Kimball TR, Tymitz KM, Penninger JM, Molkentin JD. Temporally regulated and tissue-specific gene manipulations in the adult and embryonic heart using a tamoxifen-inducible cre protein. Circulation research. 2001; 89:20–25. [PubMed: 11440973]

22. Hu P, Zhang D, Swenson L, Chakrabarti G, Abel ED, Litwin SE. Minimally invasive aortic banding in mice: Effects of altered cardiomyocyte insulin signaling during pressure overload. Am J Physiol Heart Circ Physiol. 2003; 285:H1261–H1269. [PubMed: 12738623]

23. Radke MH, Peng J, Wu Y, McNabb M, Nelson OL, Granzier H, Gotthardt M. Targeted deletion of titin n2b region leads to diastolic dysfunction and cardiac atrophy. Proc Natl Acad Sci U S A. 2007; 104:3444–3449. [PubMed: 17360664]

24. Burkhoff D, Mirsky I, Suga H. Assessment of systolic and diastolic ventricular properties via pressure-volume analysis: A guide for clinical, translational, and basic researchers. Am J Physiol Heart Circ Physiol. 2005; 289:H501–H512. [PubMed: 16014610]

25. O'Connell TD, Rodrigo MC, Simpson PC. Isolation and culture of adult mouse cardiac myocytes. Methods Mol Biol. 2007; 357:271–296. [PubMed: 17172694]

26. King NM, Methawasin M, Nedrud J, Harrell N, Chung CS, Helmes M, Granzier H. Mouse intact cardiac myocyte mechanics: Cross-bridge and titin-based stress in unactivated cells. J Gen Physiol. 2011; 137:81–91. [PubMed: 21187335]

27. Wu Y, Cazorla O, Labeit D, Labeit S, Granzier H. Changes in titin and collagen underlie diastolic stiffness diversity of cardiac muscle. J Mol Cell Cardiol. 2000; 32:2151–2162. [PubMed: 11112991]

28. Lahmers S, Wu Y, Call DR, Labeit S, Granzier H. Developmental control of titin isoform expression and passive stiffness in fetal and neonatal myocardium. Circ Res. 2004; 94:505–513. [PubMed: 14707027]
29. Hudson BD, Hidalgo CG, Gotthardt M, Granzier HL. Excision of titin's cardiac pevk spring element abolishes pkcalpha-induced increases in myocardial stiffness. J Mol Cell Cardiol. 2010; 48:972–978. [PubMed: 20026128]
30. Little WC, Ohno M, Kitzman DW, Thomas JD, Cheng CP. Determination of left ventricular chamber stiffness from the time for deceleration of early left ventricular filling. Circulation. 1995; 92:1933–1939. [PubMed: 7671378]
31. Ohno M, Cheng CP, Little WC. Mechanism of altered patterns of left ventricular filling during the development of congestive heart failure. Circulation. 1994; 89:2241–2250. [PubMed: 8181149]
32. Jacques DC, Pinsky MR, Severyn D, Gorcsan J 3rd. Influence of alterations in loading on mitral annular velocity by tissue doppler echocardiography and its associated ability to predict filling pressures. Chest. 2004; 126:1910–1918. [PubMed: 15596692]
33. Garcia MJ, Thomas JD, Klein AL. New doppler echocardiographic applications for the study of diastolic function. Journal of the American College of Cardiology. 1998; 32:865–875. [PubMed: 9768704]
34. Toischer K, Rokita AG, Unsold B, Zhu W, Kararigas G, Sossalla S, Reuter SP, Becker A, Teucher N, Seidler T, Grebe C, Preuss L, Gupta SN, Schmidt K, Lehnart SE, Kruger M, Linke WA, Backs J, Regitz-Zagrosek V, Schafer K, Field LJ, Maier LS, Hasenfuss G. Differential cardiac remodeling in preload versus afterload. Circulation. 2010; 122:993–1003. [PubMed: 20733099]
35. Perkin J, Slater R, Del Favero G, Lanzicher T, Hidalgo C, Anderson B, Smith JE 3rd, Sbaizero O, Labeit S, Granzier H. Phosphorylating titin's cardiac n2b element by erk2 or camkiidelta lowers the single molecule and cardiac muscle force. Biophysical journal. 2015; 109:2592–2601. [PubMed: 26682816]
36. Kobirumaki-Shimozawa F, Oyama K, Shimozawa T, Mizuno A, Ohki T, Terui T, Minamisawa S, Ishiwata S, Fukuda N. Nano-imaging of the beating mouse heart in vivo: Importance of sarcomere dynamics, as opposed to sarcomere length per se, in the regulation of cardiac function. The Journal of general physiology. 2016; 147:53–62. [PubMed: 26712849]
37. Granzier HL, Radke MH, Peng J, Westermann D, Nelson OL, Rost K, King NM, Yu Q, Tschope C, McNabb M, Larson DF, Labeit S, Gotthardt M. Truncation of titin's elastic pevk region leads to cardiomyopathy with diastolic dysfunction. Circ Res. 2009; 105:557–564. [PubMed: 19679835]
38. Linke WA, Hamdani N. Gigantic business: Titin properties and function through thick and thin. Circulation research. 2014; 114:1052–1068. [PubMed: 24625729]
39. Redfield MM, Chen HH, Borlaug BA, Semigran MJ, Lee KL, Lewis G, LeWinter MM, Rouleau JL, Bull DA, Mann DL, Deswal A, Stevenson LW, Givertz MM, Ofili EO, O'Connor CM, Felker GM, Goldsmith SR, Bart BA, McNulty SE, Ibarra JC, Lin G, Oh JK, Patel MR, Kim RJ, Tracy RP, Velazquez EJ, Anstrom KJ, Hernandez AF, Mascette AM, Braunwald E. Effect of phosphodiesterase-5 inhibition on exercise capacity and clinical status in heart failure with preserved ejection fraction: A randomized clinical trial. JAMA. 2013; 309:1268–1277. [PubMed: 23478662]
40. LeWinter MM, Granzier H. Cardiac titin: A multifunctional giant. Circulation. 2010; 121:2137–2145. [PubMed: 20479164]
41. Yu CM, Fung WH, Lin H, Zhang Q, Sanderson JE, Lau CP. Predictors of left ventricular reverse remodeling after cardiac resynchronization therapy for heart failure secondary to idiopathic dilated or ischemic cardiomyopathy. The American journal of cardiology. 2003; 91:684–688. [PubMed: 12633798]
42. Markowitz SM, Lewen JM, Wiggenhorn CJ, Abraham WT, Stein KM, Iwai S, Lerman BB. Relationship of reverse anatomical remodeling and ventricular arrhythmias after cardiac resynchronization. J Cardiovasc Electrophysiol. 2009; 20:293–298. [PubMed: 19175852]
43. Kartal Y, Yavuzgil O, Bozoglu M, Alp A, Can LH, Hasdemir C. Cardiac resynchronization therapy with or without anatomical reverse remodeling does not affect defibrillation threshold. Pacing Clin Electrophysiol. 2012; 35:416–421. [PubMed: 22303933]

44. Shetty AK, Duckett SG, Ginks MR, Ma Y, Sohal M, Bostock J, Kapetanakis S, Singh JP, Rhode K, Wright M, O'Neill MD, Gill JS, Carr-White G, Razavi R, Rinaldi CA. Cardiac magnetic resonance-derived anatomy, scar, and dyssynchrony fused with fluoroscopy to guide lv lead placement in cardiac resynchronization therapy: A comparison with acute haemodynamic measures and echocardiographic reverse remodelling. European heart journal cardiovascular Imaging. 2013; 14:692–699. [PubMed: 23175695]

45. Redfield MM, Borlaug BA, Lewis GD, Mohammed SF, Semigran MJ, Lewinter MM, Deswal A, Hernandez AF, Lee KL, Braunwald E. Heart Failure Clinical Research N. Phosphdiesterase-5 inhibition to improve clinical status and exercise capacity in diastolic heart failure (relax) trial: Rationale and design. Circ Heart Fail. 2012; 5:653–659. [PubMed: 22991405]

46. Redfield MM, Chen HH, Borlaug BA, Semigran MJ, Lee KL, Lewis G, LeWinter MM, Rouleau JL, Bull DA, Mann DL, Deswal A, Stevenson LW, Givertz MM, Ofili EO, O'Connor CM, Felker GM, Goldsmith SR, Bart BA, McNulty SE, Ibarra JC, Lin G, Oh JK, Patel MR, Kim RJ, Tracy RP, Velazquez EJ, Anstrom KJ, Hernandez AF, Mascette AM, Braunwald E, Trial R. Effect of phosphodiesterase-5 inhibition on exercise capacity and clinical status in heart failure with preserved ejection fraction: A randomized clinical trial. JAMA. 2013; 309:1268–1277. [PubMed: 23478662]

47. Maatz H, Jens M, Liss M, Schafer S, Heinig M, Kirchner M, Adami E, Rintisch C, Dauksaite V, Radke MH, Selbach M, Barton PJ, Cook SA, Rajewsky N, Gotthardt M, Landthaler M, Hubner N. Rna-binding protein rbm20 represses splicing to orchestrate cardiac pre-mrna processing. The Journal of clinical investigation. 2014; 124:3419–3430. [PubMed: 24960161]

Clinical perspective

What is New?

- Titin is a sarcomeric protein that functions as a molecular spring that contributes greatly to LV passive stiffness. The spring properties can be tuned through posttranscriptional and posttranslational processes and their derangement has been shown to contribute to diastolic dysfunction in patients with HFpEF (Heart Failure with preserved Ejection Fraction). Recently the titin splicing factor RBM20 was discovered and we studied whether inhibition of RBM20 can be used to improve diastolic function in a mouse model of HFpEF.
- We discovered that inactivating RBM20 results in upregulation of compliant titin isoforms and a large reduction in cellular passive stiffness whereas ECM-based stiffness is unaffected. LV diastolic chamber compliance, concentric remodeling and exercise tolerance were all improved.

What are the clinical implications?

- The prevalence of HFpEF continues to grow, but no treatment strategy has been proven to be effective. The finding that inactivating RBM20 causes expression of compliant titin isoforms and has a beneficial effect on diastolic health and exercise tolerance shows a possible pathway by which diastolic dysfunction might be ameliorated in HFpEF patients.

Titin holds promise as a therapeutic target for HFpEF

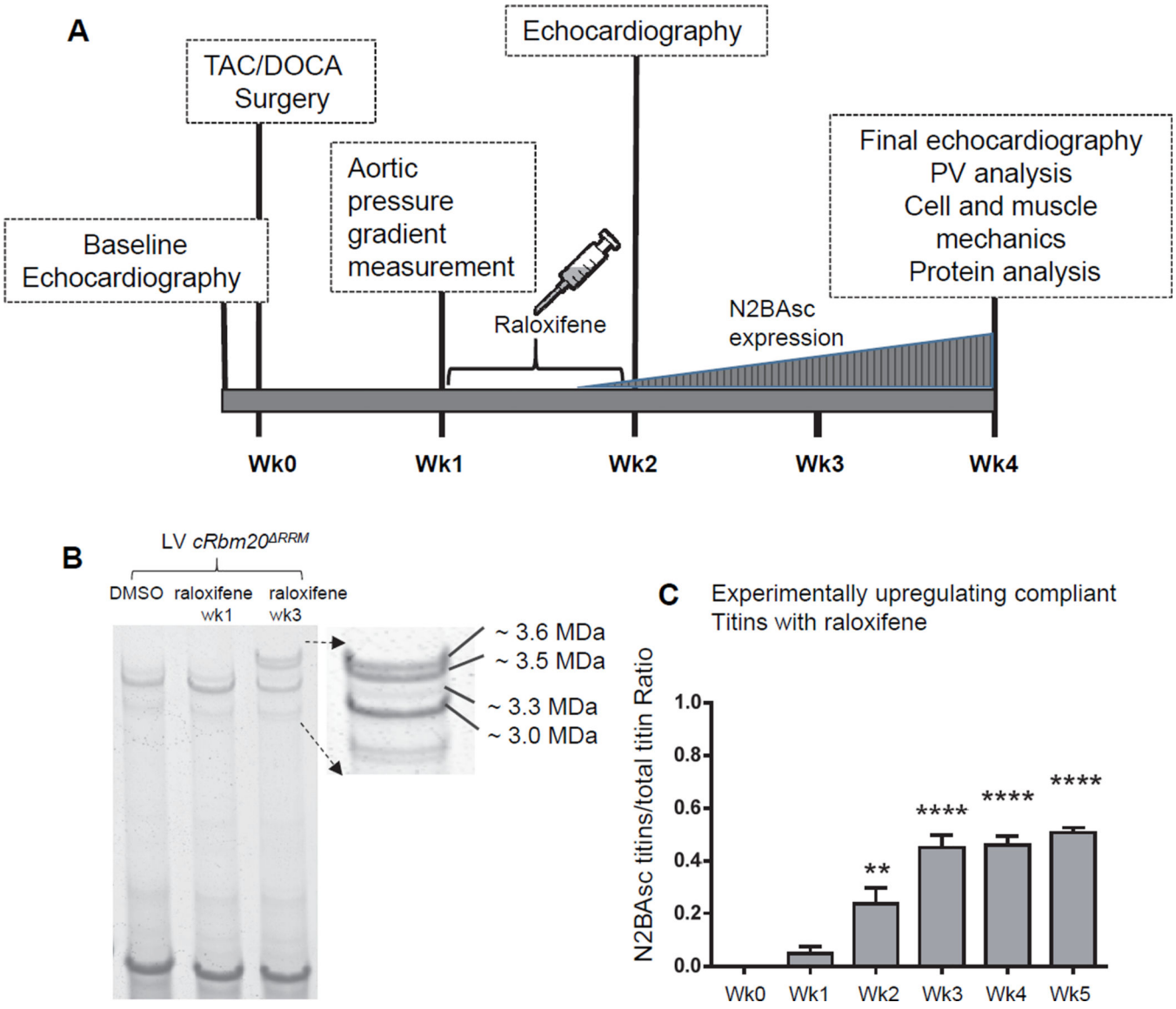

Figure 1.

A) Schematic of experimental protocol. Diastolic dysfunction was induced in *cRbm20*$^{\Delta RRM}$ mice by TAC surgery with DOCA pellet implantation. At 1 week post TAC/DOCA surgery, post constrictional aortic flow velocity was measured to quantify severity of aortic constriction. Raloxifene or DMSO (vehicle) was then administered via intraperitoneal injection daily for 8 consecutive days. At 2 weeks post TAC/DOCA surgery, echocardiography was used to evaluate cardiac morphology and study diastolic dysfunction. At 4 weeks post-surgery, a final echo analysis was performed after which the animals were utilized for PV analysis, cell/muscle mechanics or protein studies. **B) Titin isoform expression in *cRbm20*$^{\Delta RRM}$ mice after raloxifene injection**. A representative gel image shows that LV myocardium of *cRBM20*$^{\Delta RRM}$ mice treated with raloxifene expressed the normal adult N2B titin (~3.0 MDa) and N2BA titin (~3.3 MDa) isoform at 1 week, but after 3 weeks also expressed 2 very large titin isoforms (~3.5 and 3.6 MDa in size) that we named

super-compliant titin, or N2BAsc. **C)** A significant amount of N2BAsc titins was observed as early as 2 weeks after beginning of raloxifene injection. The ratio of N2BAsc / total titin reached ~ 0.45 after week 3 and then remained nearly stable. **p≤0.01, ****p≤0.0001 vs. Week 0. (n=10,5,6,6,6,4 mice for week 0,1,2,3,4,5 respectively).

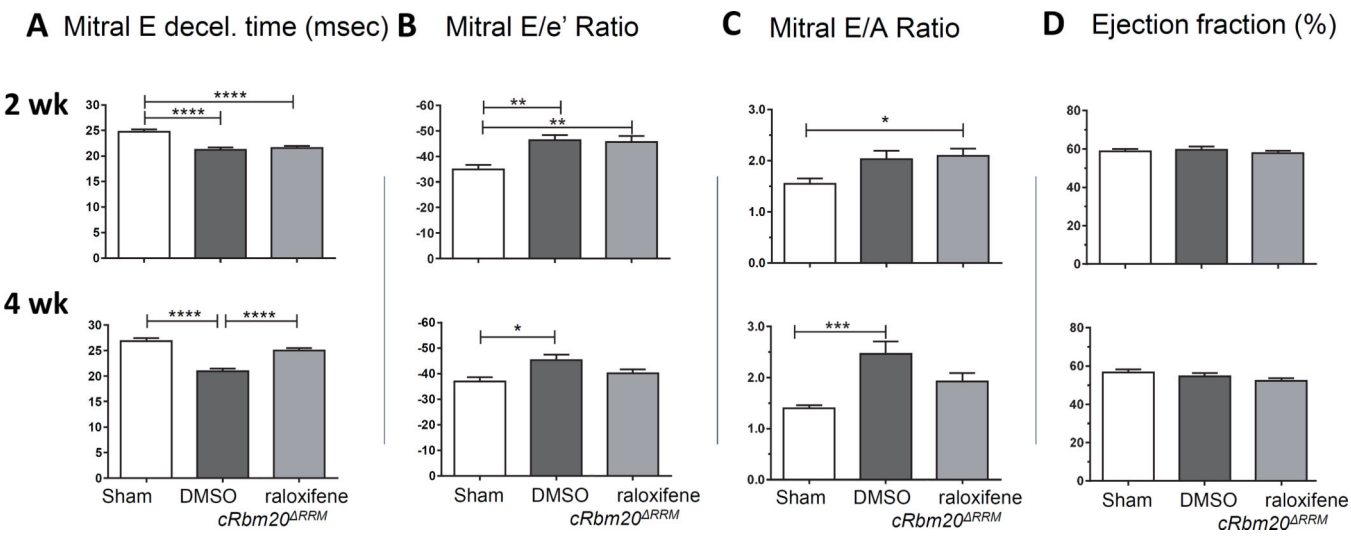

Figure 2. Diastolic (A–C) and (D) systolic function 2 weeks (top row) and 4 weeks (bottom row) after TAC/DOCA surgery: Echocardiography

Top. Mice have diastolic dysfunction 2 weeks after TAC/DOCA surgery. *cRbm20*$^{\Delta RRM}$ TAC/DOCA mice were studied that had received 1 week post-surgery DMSO (control) or raloxifene (note that the one week period from start of injection to echo analysis is insufficient for N2BAsc expression). Both TAC/DOCA groups had a reduced mitral E deceleration time **(A)**, increased mitral E/e' ratio **(B)** and increased E/A ratio **(C)**, all indicating diastolic dysfunction. The ejections fraction **(D)** is normal. **Bottom**. Recovery of diastolic dysfunction in *cRbm20*$^{\Delta RRM}$-raloxifene mice 4 weeks after TAC/DOCA surgery. (Note that the 3 week period from start of raloxifene injection to echo analysis results in an optimal N2BAsc expression level in *cRbm20*$^{\Delta RRM}$-raloxifene mice.) The *cRbm20*$^{\Delta RRM}$-DMSO group had (compared to sham) a reduced mitral E deceleration time, increased mitral E/e' ratio and increase E/A ratio, all of which indicate diastolic dysfunction. The *cRbm20*$^{\Delta RRM}$-raloxifene group had normalized diastolic parameters. The ejection fraction was normal in both TAC/DOCA groups. * p≤0.05; **p≤0.01, ***p≤0.001; ****p≤0.0001. (n=20 sham, 29 *cRbm20*$^{\Delta RRM}$-DMSO, and 37 *cRbm20*$^{\Delta RRM}$-raloxifene mice.)

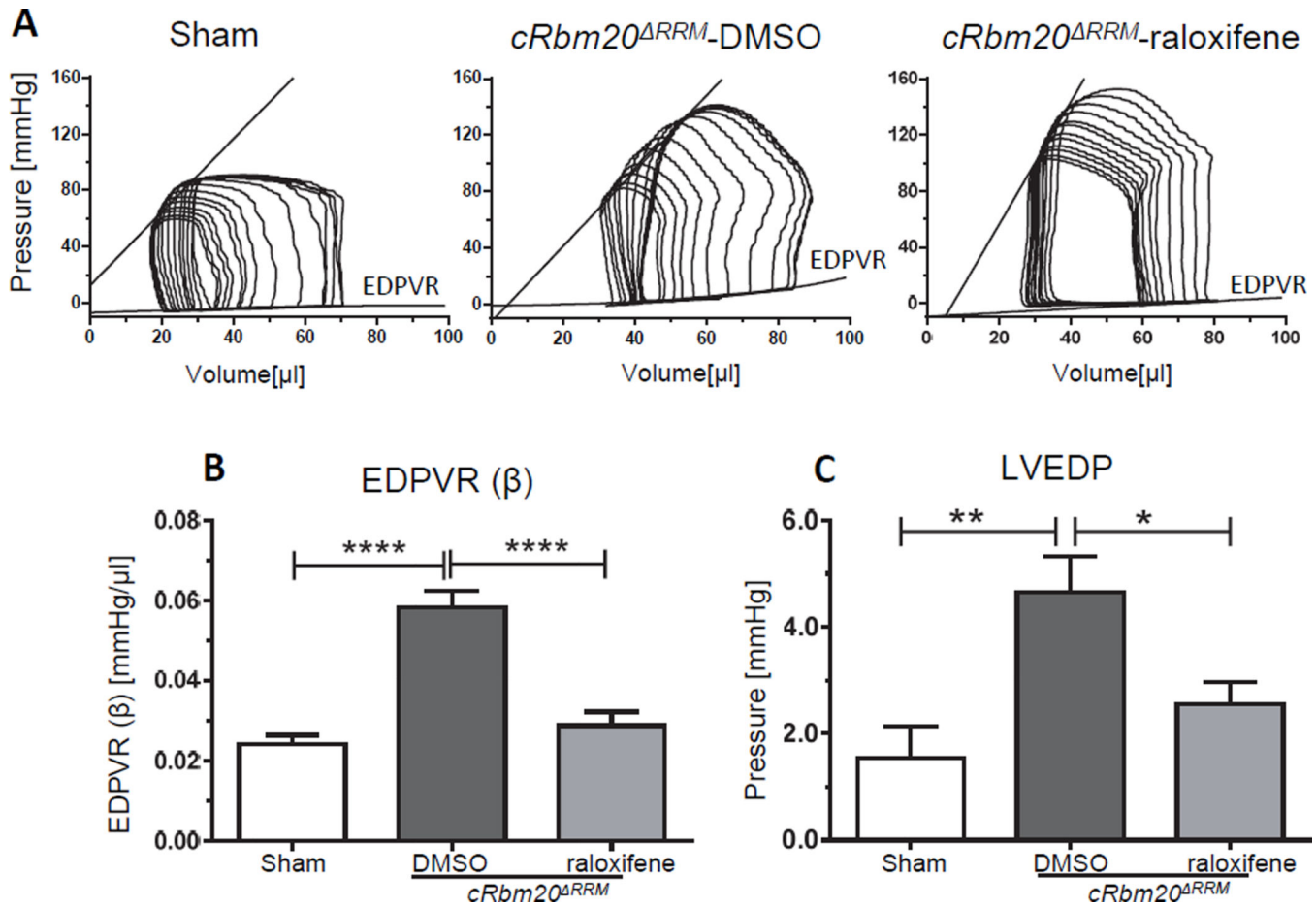

Figure 3. Recovery of diastolic dysfunction in *cRbm20*$^{\Delta RRM}$-raloxifene mice 4 weeks after TAC/DOCA surgery: Pressure-Volume analysis

DMSO (control) and raloxifene TAC/DOCA *cRbm20*$^{\Delta RRM}$ mice were studied by PV analysis. **A)** Representative examples of PV loops. PV analysis was performed on anesthetized and ventilated mice under isoflurane. Inferior vena caval occlusions were conducted to assess load-independent parameters. **(B)** Diastolic stiffness coefficient β of EDPVR was significantly increased in the *cRbm20*$^{\Delta RRM}$-DMSO group but was normal in *cRbm20*$^{\Delta RRM}$-raloxifene group. **(C)** LVEDP was elevated in *cRbm20*$^{\Delta RRM}$-DMSO mice. * p≤0.05; **p≤0.01; ****p≤0.0001. (n=12 sham, 21 *cRbm20*$^{\Delta RRM}$-DMSO, 28 *cRbm20*$^{\Delta RRM}$-raloxifene)

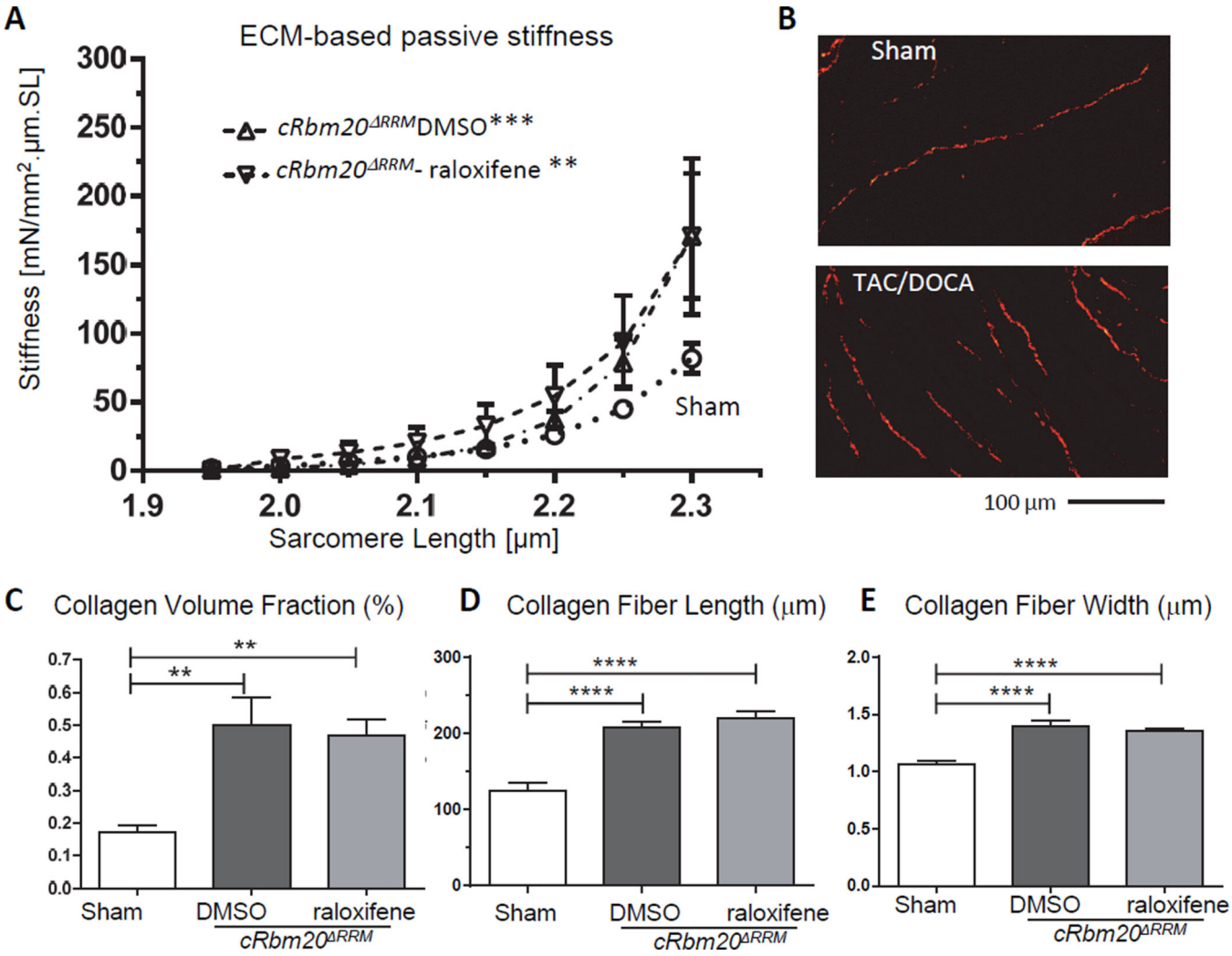

Figure 4. Characteristics of the extracellular matrix (ECM)

(A) ECM-based myocardial passive stiffness of muscle strips from LV free wall. The relation of ECM-based stiffness vs. SL of sham (circle), *cRbm20*$^{\Delta RRM}$-DMSO (upward triangle) and *cRbm20*$^{\Delta RRM}$-raloxifene (inverted triangle) are shown. ECM-based stiffness was increased in both TAC/DOCA groups. (For analysis, see Supplemental Methods). **p≤0.01; ***p≤0.001 vs. Sham. (n=6, 6, 6 muscle strips from 4, 5, 6 mice for ECM-based passive stiffness.) **(B–E)** Quantification of collagen in LV myocardium. **(B)** Representative PSR staining for collagen of LV myocardium. Quantitative analysis showed a similarly increase in collagen volume fraction **(C)**, collagen fiber length **(D)**, and collagen fiber width **(E)** in both TAC/DOCA groups. **p≤0.01; ****p≤0.0001. (n=9, 14, 21 mice for collagen quantification.)

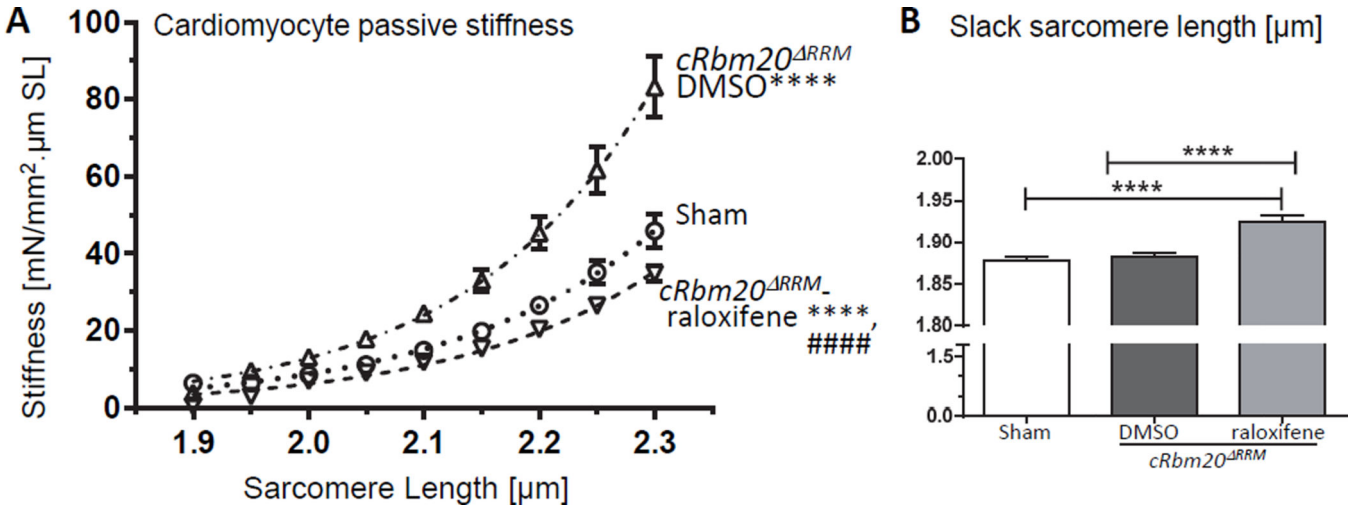

Figure 5. Cardiomyocyte (LV) passive stiffness and slack sarcomere length

(A) Skinned cardiomyocyte passive stiffness was increased in *cRbm20*$^{\Delta RRM}$-DMSO but was reduced in *cRbm20*$^{\Delta RRM}$-raloxifene mice. (For analysis, see Supplemental Methods.) ****p≤0.0001 vs. Sham; $^{\#\#\#\#}$p≤0.0001 vs. *cRbm20*$^{\Delta RRM}$-DMSO. **(B)** Slack sarcomere length of skinned cardiomyocytes (see text for details). ****p≤0.0001 (n=13, 15, 19 cells from 6, 6, 7 mice).

A

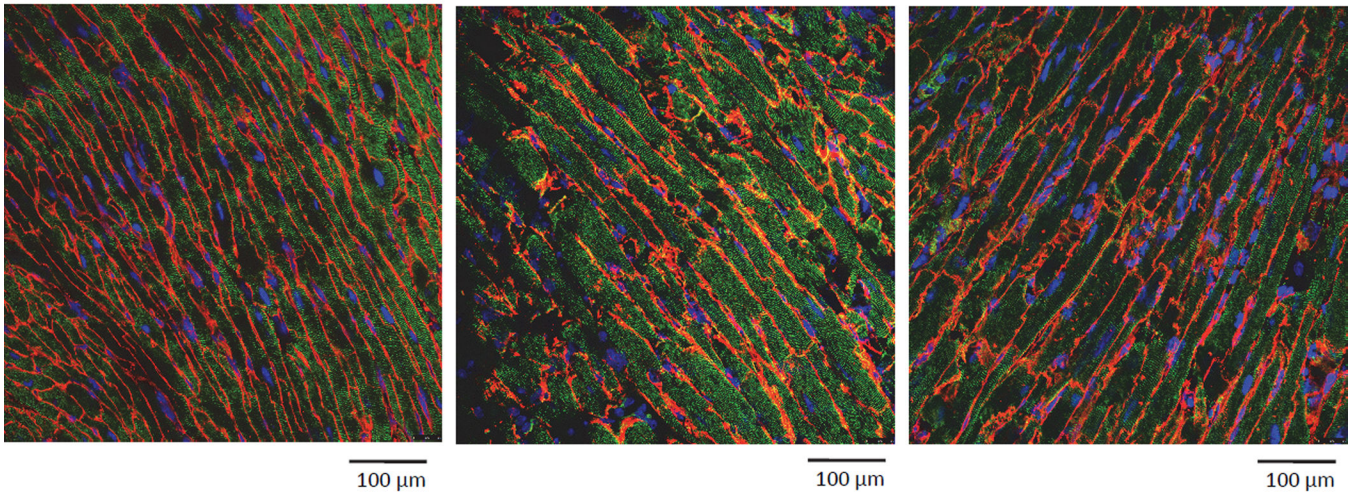

B

	Dimension of cardiomyocytes			Sarcomere length[μm]
	Length[μm]	Width[μm]	Area [μm^2]	
Sham	110.5±1.0	23.1±0.2	1,863±25.7	1.88±0.02
cRbm20$^{\Delta RRM}$-DMSO	121.7±1.2****	27.8±0.2****	2,499±34.6****	1.87±0.02
cRbm20$^{\Delta RRM}$-raloxifene	118.6±1.0****	26.6±0.2****, ###	2,320±26.5**** ,####	1.96±0.02**, ##

Figure 6. Cardiomyocyte dimensions at diastasis

(A) Representative confocal immunofluorescent images of LV wall tissue at diastasis. Red: laminin and connexin43, green: alpha-actinin, and blue: nucleus. **(B) Comparison of cell dimension in sham and two TAC/DOCA groups (DMSO and raloxifene)**. Cardiomyocytes of both TAC/DOCA groups are longer and wider than in sham and consequently have a larger area. However, cardiomyocytes of *cRbm20*$^{\Delta RRM}$-raloxifene are smaller than *cRbm20*$^{\Delta RRM}$-DMSO. SL of *cRbm20*$^{\Delta RRM}$-raloxifene is longer than sham and *cRbm20*$^{\Delta RRM}$-DMSO. **p≤0.01, ****p≤0.0001 vs. Sham;$^{\#\#}$p≤0.01, $^{\#\#\#}$p≤0.001, $^{\#\#\#\#}$p≤0.0001 vs. *cRbm20*$^{\Delta RRM}$-DMSO group. (n= 631, 580, 634 cells for cell dimension and 75, 79, 93 cells for SL measurement in 4, 4, 3 hearts).

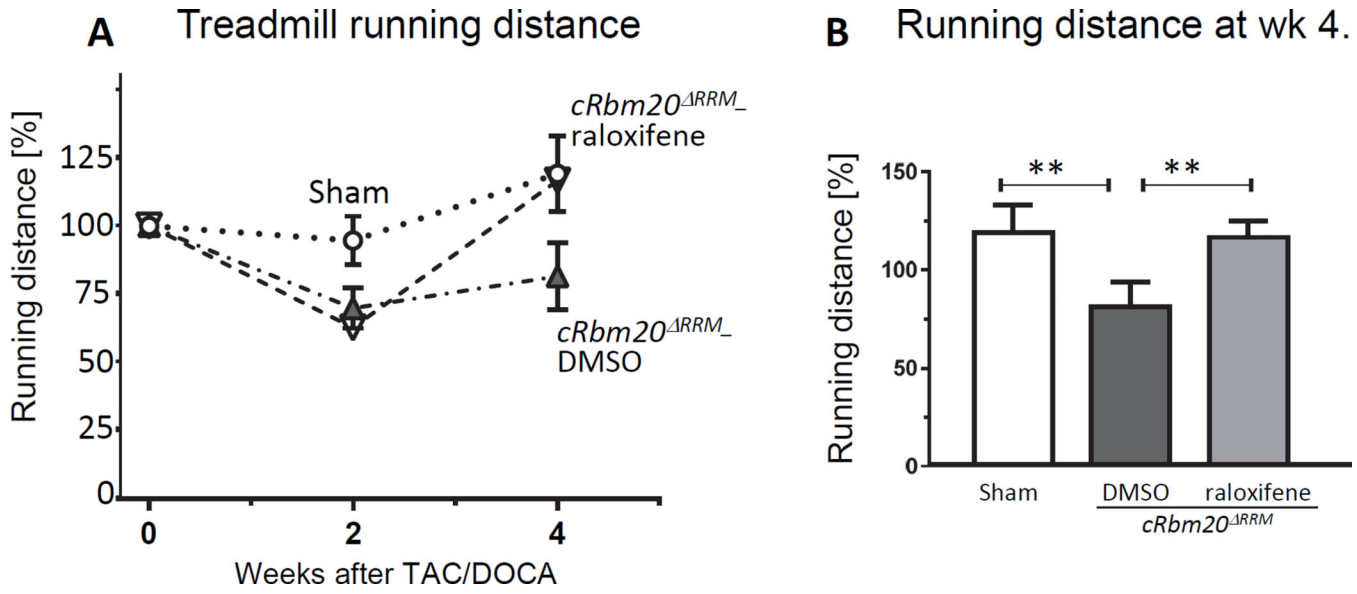

Figure 7. Exercise tolerance study

(A) Exercise tolerance was evaluated by measuring the running distance in a treadmill running test at three times: preoperative and at 2 weeks and at 4 weeks post TAC/DOCA surgery. The running distance was calculated as a percent of the preoperative running distance of each individual mouse. Sham (circle), *cRbm20*$^{\Delta RRM}$-DMSO (upward triangle) and *cRbm20*$^{\Delta RRM}$-raloxifene (inverted triangle). **(B)** At 4 weeks post-surgery (after expression of N2BAsc titin in the raloxifene group), the *cRbm20*$^{\Delta RRM}$-raloxifene mice showed a significantly increased running distance compared to *cRbm20*$^{\Delta RRM}$-DMSO mice. (For analysis, see Supplemental Methods.) **p≤0.01. (n= 7 sham, 10 *cRbm20*$^{\Delta RRM}$-DMSO, 10 *cRbm20*$^{\Delta RRM}$-raloxifene mice).

Table 1

Echocardiographic parameters, pressure volume analysis parameters and tissue morphometry at 4 weeks post TAC/DOCA surgery (with expression of N2BAsc titins in the *cRbm20*$^{\Delta RRM}$-raloxifene group).

At 4 weeks post-surgery	**Sham**	***cRbm20*$^{\Delta RRM}$ --DMSO**	***cRbm20*$^{\Delta RRM}$ --raloxifene**
Age (days)	85 ± 2	84 ± 2	84 ± 1
Body Weight, BW (gm)	23.7 ± 0.6	25.7 ± 0.5*	24.3 ± 0.3$^{\#}$
Tibial Length, TL(mm)	17.0 ± 0.1	17.0 ± 0.1	17.0 ± 0.1
Echocardiography			
Heart Rate (bpm)	517 ± 13	501 ± 16	501 ± 7
LVID;d (mm)	3.85 ± 0.06	4.02 ± 0.06	4.15 ± 0.06**
WT;d (mm)	0.80 ± 0.05	0.98 ± 0.02**	0.95 ± 0.02
LVID;s (mm)	2.72 ± 0.06	2.90 ± 0.08	3.05 ± 0.08*
WT;s (mm)	1.05 ± 0.06	1.29 ± 0.02****	1.26 ± 0.02***
Eccentricity	4.6 ± 0.2	4.1 ± 0.1**	4.4 ± 0.1
EF (%)	56.8 ± 1.4	54.5 ± 1.8	52.2 ± 1.5
LA dimension (mm)	2.13 ± 0.03	2.46 ± 0.02****	2.43 ± 0.03****
E decel time (ms)	26.8 ± 0.6	20.9 ± 0.5****	25.0 ± 0.5$^{\#\#\#\#}$
MV E/A	1.40 ± 0.06	2.46 ± 0.24***	1.93 ± 0.16
MV E/é	−36.9 ± 1.7	−45.3 ± 2.2*	−40.2 ± 1.6
Pressure-Volume Analysis			
Load Dependent Parameters			
ESP (mmHg)	96 ± 2	128 ± 3****	128 ± 3****
EDP (mmHg)	1.6 ± 0.6	4.7 ± 0.7**	2.5 ± 0.4$^{\#}$
dPmax (mmHg/s)	10,101 ± 426	9,089 ± 530	9,145 ± 488
dPmin (mmHg/s)	−10,091 ± 567	−9,870 ± 468	−10,621 ± 475
ESV (μl)	24 ± 2	39 ± 3**	41 ± 2**
EDV (μl)	63 ± 4	75 ± 3	80 ± 3**
SV (μl)	39 ± 2	37 ± 1	39 ± 2
Tau Glantz (ms)	8.2 ± 0.5	11.5 ± 0.6**	10.2 ± 0.7
Ea (mmHg/μl)	2.5 ± 0.1	3.7 ± 0.1***	3.6 ± 0.2**
Load Independent Parameters			
Ees (mmHg/μl)	4.01 ± 0.38	4.49 ± 0.53	3.39 ± 0.25
PRSW (mmHg)	95.3 ± 3.5	107.6 ± 7.4	105.4 ± 5.3
EDPVR(mmHg/μl)	0.024 ± 0.002	0.059 ± 0.004****	0.029 ± 0.003$^{\#\#\#\#}$
Tissue Morphometry			
LV/TL (mg/mm)	4.85 ± 0.10	7.31 ± 0.32****	6.92 ± 0.27***

At 4 weeks post-surgery	**Sham**	***cRbm20*$^{\Delta RRM}$ --DMSO**	***cRbm20*$^{\Delta RRM}$ --raloxifene**
RV/TL (mg/mm)	1.23 ± 0.05	1.32 ± 0.05	1.31 ± 0.04
Lt ATR/TL (mg/mm)	0.21 ± 0.01	0.36 ± 0.03	0.37 ± 0.04 *
Rt ATR/TL (mg/mm)	0.14 ± 0.02	0.23 ± 0.01 **	0.20 ± 0.01 *
Lung/TL (mg/mm)	8.55 ± 0.22	9.45 ± 0.27 *	9.16 ± 0.17

LV, left ventricle; d,diastole; s,systole; LVID, LV internal dimension; WT, wall thickness; Eccentricity indicates LVIDd/WTd; Vol, volume; SV, stroke volume;FS, fractional shortening; EF, ejection fraction; LA, left atrium; MV, mitral valve. ESP: end-systolic pressure; EDP: end-diastolic pressure; dPmax:maximal rate of pressure change; dPmin:minimal rate of pressure change; ESV: end-systolic volume; EDV: end-diastolic volume; SV: stroke volume; EF: ejection fraction; Tau Glantz: LV relaxation time constant ; Ea: effective arterial elastance; Ees: end systolic elastance; PRSW: preload recruitable stroke work; EDPVR: end diastolic pressure volume relation; HW: whole heart weight; RV: right ventricle; ATR: atria. TL: tibial length.

*p≤0.05,

**p≤0.01,

***p≤0.001,

****p≤0.0001 vs. Sham;

#p≤0.05,

####p≤0.0001 vs. *cRbm20*$^{\Delta RRM}$-DMSO group. (n=10,29,37 mice for echocardiography, n=12,21,28 mice for PV analysis, n=12,22,29 mice for tissue morphometry)